fermentation

MDPI

Article

Genomic Insight and Optimization of Astaxanthin Production from a New *Rhodotorula* sp. CP72-2

Engkarat Kingkaew [1], Nisachon Tedsree [2], Sukanya Phuengjayaem [3], Pornchai Rojsitthisak [4], Boonchoo Sritularak [5], Worathat Thitikornpong [4], Somphob Thompho [6], Wuttichai Mhuantong [7] and Somboon Tanasupawat [1,*]

1 Department of Biochemistry and Microbiology, Faculty of Pharmaceutical Sciences, Chulalongkorn University, Bangkok 10330, Thailand; engkarat.k@chula.ac.th
2 Faculty of Science and Arts, Burapha University, Chanthaburi Campus, Chanthaburi 22170, Thailand; nisachon@go.buu.ac.th
3 Department of Microbiology, Faculty of Science, King Mongkut's University of Technology Thonburi, Bangkok 10140, Thailand; sukanya.phu@kmutt.ac.th
4 Department of Food and Pharmaceutical Chemistry, Faculty of Pharmaceutical Sciences, Chulalongkorn University, Bangkok 10330, Thailand; pornchai.r@chula.ac.th (P.R.); worathat.t@pharm.chula.ac.th (W.T.)
5 Department of Pharmacognosy and Pharmaceutical Botany, Faculty of Pharmaceutical Sciences, Chulalongkorn University, Bangkok 10330, Thailand; boonchoo.sr@chula.ac.th
6 Pharmaceutical Research Instrument Center, Faculty of Pharmaceutical Sciences, Chulalongkorn University, Bangkok 10330, Thailand; somphob.t@chula.ac.th
7 National Center for Genetic Engineering and Biotechnology (BIOTEC), National Science and Technology Development Agency (NSTDA), Khlong Luang 12120, Thailand; wuttichai.mhu@biotec.or.th
* Correspondence: somboon.t@chula.ac.th; Tel.: +66-2-218-8376; Fax: +66-2-254-5195

Abstract: Astaxanthin is a carotenoid pigment extensively used in various industries. *Rhodotorula* sp. CP72-2, isolated from *Calotropis gigantea*, showed potential astaxanthin production. In this study, strain CP72-2 was identified as a putative new species in the genus *Rhodotorula* based on the 26S rRNA gene sequence (98% identity). It was first used as the microbial source for producing astaxanthin. Strain CP72-2 was screened for its astaxanthin production and was identified and quantified by High-Performance Liquid Chromatography (HPLC), Liquid Chromatography-Mass Spectrometry (LC-MS), and UV-Vis spectrophotometer. After a screening of astaxanthin production, various carbon sources, pH, temperature, and incubation period were evaluated for their effect on the astaxanthin production of strain CP72-2. Among the several experimental factors, the most efficient conditions for astaxanthin production were glucose (50 g/L), pH 4.5, 25 °C, and three days of cultivation. The assembly genome of strain CP72-2 has a total length of 21,358,924 bp and a GC content of 64.90%. The putative candidate astaxanthin biosynthesis-associated genes (i.e., *CrtE*, *CrtYB*, *CrtI*, *CrtS*, *CrtR*, *CrtW*, *CrtO*, and *CrtZ*) were found. This research presents the first report on the production and optimization of astaxanthin from strain CP72-2 and its genome analysis, focusing on the biotechnological potential of the astaxanthin producer.

Keywords: yeast; *Rhodotorula*; biotechnological potential; astaxanthin production; optimization; genomic analysis

Citation: Kingkaew, E.; Tedsree, N.; Phuengjayaem, S.; Rojsitthisak, P.; Sritularak, B.; Thitikornpong, W.; Thompho, S.; Mhuantong, W.; Tanasupawat, S. Genomic Insight and Optimization of Astaxanthin Production from a New *Rhodotorula* sp. CP72-2. *Fermentation* **2023**, *9*, 501. https://doi.org/10.3390/fermentation9060501

Academic Editor: Hao Li

Received: 14 April 2023
Revised: 18 May 2023
Accepted: 22 May 2023
Published: 24 May 2023

1. Introduction

Coloration is fundamental in various industries, including pharmaceuticals, food, cosmetics, and healthcare; pigments are often the key ingredients used for this purpose. Pigments are crucial in the food industry [1]. Their specific origin determines their operational, functional, and health properties, thus shaping their importance and application in food production. Natural and chemical processes are the two methods for obtaining

pigments in the food industry [2]. While chemical pigment production may suffer from several limitations, such as by-products with adverse environmental effects and the potential for toxicity, natural resources obtained from plants, animals, and microorganisms that can produce pigments on a large scale offer a viable alternative. As such, consumers are now inclined to prefer natural pigments over their artificial counterparts [1]. Utilizing novel colors derived from biotechnology produced by microorganisms presents a promising and sophisticated solution for meeting this demand.

Astaxanthin (3,3′-dihydroxy-β, β-caroten-4,4′-dione), an oxygenated carotenoid, displays a vivid spectrum of colors ranging from yellow to red and is coveted across multiple industries, including aquaculture, cosmetics, pharmaceuticals, food, feed, and medicine, for its remarkable health-promoting properties. This naturally occurring pigment is a potent antioxidant, anti-inflammatory, and anticancer agent, conferring a wide array of benefits for the eye, heart, liver, skin, and immune system [3–6]. Although several microorganisms can synthesize astaxanthin [2], *Haematococcus pluvialis* has become the most significant commercial source [7]. However, the practical implementation of *H. pluvialis* is limited by its lengthy autotrophic cultivation process and the necessity of disrupting the cell wall for astaxanthin extraction. In contrast, *Xanthophyllomyces dendrorhous*, a red yeast previously known as *Phaffia rhodozyma*, shows promise as a desirable alternative for astaxanthin production [2,8]. Notably, yeasts offer several advantages over microalgae, including rapid growth rates, independence from changing climatic and seasonal conditions, no land space requirements for cultivation, and the ability to utilize various carbon sources. Additionally, *X. dendrorhous* can accumulate astaxanthin in its cytoplasmic membrane, precluding the need for cell wall disruption during extraction [9].

Astaxanthin production is a significant factor in determining the economic viability of the process. In order to reduce the production costs of astaxanthin and optimize the cultivation medium and conditions, basic research has been conducted to improve the process for industrial applications. Utilizing the One-Factor-At-A-Time (OFAAT) technique is a highly efficacious approach to optimizing astaxanthin levels and mitigating the inherent variability in its quantity. The OFAAT technique allows for systematically exploring individual factors and their impact on the targeted outcome, ultimately leading to an enhanced understanding of the underlying mechanisms and their interplay. Therefore, the OFAAT technique can provide a robust and reliable means of achieving optimal astaxanthin production with reduced variance, thereby ensuring a more consistent and high-quality end product. In this context, our study presents the OFFAT approach to investigate astaxanthin production, optimize its yield, and focus on the astaxanthin biosynthesis-associated genes of *Rhodotorula* sp. CP72-2. Notably, this study aims to address the knowledge gap by investigating the whole-genome sequencing and optimization of astaxanthin production, which has yet to be published. Additionally, this study identified a strain, CP72-2, in the Thai Crown Flower (*Calotropis gigantea*), which presents a promising source for discovering a candidate astaxanthin-producing strain. Our study provides an innovative and comprehensive approach to astaxanthin production and will contribute to advancing the field of natural pigment production.

2. Materials and Methods

2.1. Characterization of Strain CP72-2

Rhodotorula sp. CP72-2 was isolated from the Crown Flower (*Calotropis gigantea*) in Prachinburi province, Thailand. The inoculum was cultivated in Erlenmeyer flasks of 250 mL, which contained 50 mL of Yeast extract–Malt extract (YM) medium (in g/L deionized water): peptone (bacteriological) (5.0), malt extract (3.0), yeast extract (3.0), glucose (10.0). The pH of the YM medium was adjusted to 5.5, and the cultivation was carried out on a temperature-controlled orbital shaker at 25 °C with a rotation speed of 200 rpm for 48 h.

2.1.1. Phenotypic Characteristics

The morphological and biochemical characteristics of the strain CP72-2 were determined and compared to the description of type strains [10]. Yeast cell morphology was observed using light microscopy, while the colony morphology, including the texture, color, surface, elevation, and margin, was visually recorded. Carbon assimilation tests were conducted using the ID 32 C kit (BioMerieux, Marcy-l'Étoile, France), following the manufacturer's instructions.

2.1.2. Genotypic Characteristics

Genomic DNA Extraction

To extract the genomic DNA from the strain CP72-2, a loop full of yeast cells was suspended in 200 µL of lysis buffer (100 mM Tris (pH 8.0), 30 mM EDTA (pH 8.0), 0.5% SDS) and then boiled in a water bath for 15 min. Following this, 200 µL of 2.5 M potassium acetate (pH 7.5) was added, mixed, and rapidly cooled on ice for 1 h. The supernatant was collected by centrifugation at 13,000 rpm for 5 min at 4 °C and extracted twice with 1 volume of $CHCl_3$-isoamyl alcohol (24:1, v/v). After centrifugation at 13,000 rpm for 5 min, the resulting supernatant was mixed with 1 volume of cold isopropanol and then centrifuged at 14,500 rpm for 16 min at 4 °C. The DNA pellet was washed with 70% and 90% ethanol, then centrifuged (14,500 rpm, 4 °C for 16 min). The washed DNA pellet was dried at 37 °C, dissolved in 30 µL of sterile nano pure water, and kept at −20 °C until used.

Sequencing of the 26S rRNA Gene (D1/D2 Domain)

The LSUD1/D2 domain of the 26S rRNA gene was amplified through PCR using the NL1 (5′-GCATATCAATAAGCGGAGGAAAAG-3′) and NL4 (5′-GGTCCGTGTTTCAAGACGG-3′) primers [11]. The PCR reaction consisted of a 20 µL volume containing 2 µL of DNA template, 0.4 µL of each primer (10 pmol/µL), 10 µL of 2X Go Tag green, and 7.2 µL of distilled water. The reaction was subjected to thermocycling at 94 °C for 3 min, followed by 36 cycles of 94 °C, 52 °C, and 72 °C for 30 s each, and a final extension at 72 °C for 5 min. The PCR product was purified using the Gel/PCR DNA fragment extraction kit (Geneaid Biotech Ltd., New Taipei, Taiwan). The purified PCR products were sequenced in both directions using the BT sequencing technique (Celemics, Inc., Seoul, Republic of Korea) and blasted against the NCBI database.

Genome Sequencing, Gene Prediction, and Functional Annotation

The genome of *Rhodotorula* sp. CP72-2 was sequenced using Illumina Hiseq Xten/Novaseq/MGI2000 platforms. The reads were quality controlled and then assembled using Velvet. Gap-filling was performed with SSPACE and GapFiller [12–16]. Coding genes in the genome were identified using the Augustus gene-finding software (version 3.3) [17]. Transfer RNAs (tRNAs) were detected using the program tRNAscan-SE with default parameter settings [18], and rRNA was identified using Barrnap. Other RNAs were identified using the RNA families database (rfam). The ANI value between strain CP72-2 and closely related species was calculated using FASTANI (version 1.3) [19]. The circular genomic map and Venn diagram were generated using the Prokee server [20] and Orthovenn2 web-based tool [21].

The coding genes were annotated with the National Center for Biotechnology Information (NCBI), and their functions were annotated using the Kyoto Encyclopedia of Genes and Genomes (KEGG) [22] and KOfamKOALA tools [23]. Identification of carbohydrate-active enzymes was performed using the dbCAN meta server (https://bcb.unl.edu/dbCAN2/blast.php: accessed on 13 April 2023) with HMMER: biosequence analysis with profile hidden Markov models (version: 3.3.2), and all data generated in dbCAN were based on the family classification from the CAZy database (http://www.cazy.org/: accessed on 13 April 2023) [24,25].

The assembled genome was deposited in DDBJ/ENA/GenBank under accession no. PRJNA938253.

2.2. Cultivation for Astaxanthin Production

A loopful of strain CP72-2 grown on YM agar was transferred into 50 mL of YM broth in a 250 mL flask and incubated at 25 °C with shaking at 200 rpm for 24 h. After that, 5 mL of the culture was inoculated into 45 mL of YM broth in a 250 mL flask and incubated at the same conditions for 72 h. The cells were harvested by centrifugation at 7830 rpm at 4 °C for 10 min, washed twice with distilled water, and lyophilized to determine the biomass's dry cell weight (DCW). The lyophilized cells were then used for further analysis of astaxanthin.

2.2.1. Qualitative Analysis for Astaxanthin Production by Thin-Layer Chromatography (TLC), High-Performance Liquid Chromatography (HPLC), and Liquid Chromatography-Mass Spectrometry (LC-MS)

TLC Identification

The astaxanthin extraction and qualitative analysis were performed using slightly modified methods described by Ushakumari and Ramanujan [26]. Firstly, 0.01 g DCW of lyophilized cells were suspended in 1 mL of acetone and homogenized using a pestle motor at room temperature for 3 min. Then, the supernatant was collected by centrifugation at 14,000 rpm for 10 min. A 20 µL aliquot of the extracted sample was applied to a TLC silica gel G plate using capillary and standard astaxanthin (Dayang Chem Co., Ltd., Hangzhou, China). The mobile phase for spot development was a mixture of acetone and hexane at a ratio of 1:3 (*v*/*v*). The appearance of colored bands was directly observed after development and compared with the standard astaxanthin band under visible light. Additionally, the R_f value was calculated to quantify the movement of the materials along the plate.

HPLC Identification

The lyophilized cells of *Rhodotorula* sp. CP72-2 (0.05 g DCW) were suspended in 5 mL of DMSO, mixed, sonicated at 37 kHz (Elmasonic E60H, Elma Schmidbauer GmbH, Singen, Germany) at 55 °C for 5 min, and centrifuged at 5000 rpm at 25 °C for 10 min. The resultant supernatant was filtered through a 0.22-µm membrane filter. The filtered sample was subjected to analysis by HPLC. The astaxanthin was identified using HPLC, with slight modifications [27]. A UHPLC Nexera X2 (Shimadzu, Kyoto, Japan) was equipped with an LC-30AD binary pump, an SIL-30AC autosampler, a CTO-20AC column oven, and an SPD-M30A detector. The system was computer controlled and installed with a Lab Solutions chromatography workstation to analyze data. The chromatographic column (GL Science InertSustain C18 column (4.6 mm × 150 mm, 5 µm)) was used to separate astaxanthin. The flow rates were 0.5 mL/min (0.00 to 03.00 min) and 1.0 mL/min (03.01 to 20.00 min), the detection wavelength was 480 nm, the column temperature was 30 °C, and the injection volume was 5 µL. Mobile phase A consisted of methanol/acetonitrile/ethyl acetate/formic acid (75.9:12:12:0.1, *v*/*v*), and mobile phase B consisted of methanol.

LC-MS Identification

The astaxanthin identification was conducted using LC-MS as previously described, with slight modifications [27]. Liquid Chromatography-Mass Spectrometry (LC-QqQ; LC-Triple quadrupole) was used to obtain the mass spectrum of the pigment. Initially, the sample was run through the UHPLC-Nexera series and detected with a triple quadrupole mass spectrometer (LCMS-8060NX, Shimadzu, Japan) using an InertSustain C18 column (150 mm × 4.6 mm i.d., 5 µm, GL Sciences, Tokyo, Japan) for separation. Ten microliters of the sample was injected into the column, maintained at an oven temperature of 30 °C, and eluted with a mobile phase A consisting of methanol, acetonitrile, and ethyl acetate (76:12:12, *v*/*v*), and mobile phase B consisted of methanol. The flow rate was kept constant at 1.0 mL/min.

The triple quadrupole mass spectrometer was used to detect analytes with Electron Spray Ionization (ESI) in negative mode, using optimization settings that included N_2 nebulizing gas flow at 3 L/min, heating gas flow at 15 L/min, drying gas flow at 6 L/min, interface temperature at 350 °C, DL temperature at 250 °C, and heat block temperature at

350 °C. The optimization of the MS/MS parameter for astaxanthin detection was performed in MRM mode (MS/MS) by selecting a precursor ion of 595.3822 [M-H]- and 3 product ions of 513.2000, 430.7500, and 348.9000 with Collision Energy (CE) at 25.0, 12.0, and 48.0, respectively. All extracted samples were analyzed by MS negative scan mode (MS) and recorded mass per charge (m/z) from 100 to 2000 Da.

2.2.2. Quantification Analysis of Astaxanthin Production

The methods previously described, with slight modifications, were used to extract and measure astaxanthin [28]. To extract the intracellular carotenoid content, 50 mg of lyophilized cells were suspended in 5 mL of DMSO (Sigma-Aldrich, St. Louis, MI, USA), ultrasonicated at 37 kHz and 50 °C for 30 min (Elmasonic, E60H model, Munich, Germany), and then centrifuged at 14,000 rpm and 4 °C for 40 min. The resulting cell extract was then centrifuged at 14,000 rpm for 5 min, and the extraction process was repeated until the supernatant became colorless. The concentration of astaxanthin was determined using a Cary 60 UV-Vis spectrophotometer (Agilent) at 530 nm against the pure DMSO blank [7,28]. A standard curve of absorbance versus astaxanthin concentrations was generated using the following concentrations: 0, 0.25, 0.5, 1, 2, 4, 6, and 8 µg/mL in DMSO. Astaxanthin concentration was calculated using the equation of the astaxanthin standard calibration curve (R^2 = 1.0), and the results were reported as the mean of triplicate measurements.

2.3. Optimization of Astaxanthin Production

A study was conducted to investigate the production of astaxanthin by *Rhodotorula* sp. CP72-2. The strain CP72-2 was initially inoculated on YM agar and then incubated at 25 °C for 48 h. One loop culture was transferred into a 250 mL Erlenmeyer flask containing 50 mL YM broth and then incubated at 25 °C with 200 rpm shaking for 24 h. The cells were harvested by centrifugation at 7830 rpm at 4 °C for 10 min. The resulting cell pellet was washed twice and re-suspended in a 0.85% (w/v) NaCl solution. The yeast suspension was adjusted to achieve a cell suspension with an OD_{660} of 1.00 ± 0.1 for use as an inoculum starter for investigating the optimization of astaxanthin production. Fermentation experiments were carried out in 250 mL Erlenmeyer flasks containing 50 mL of astaxanthin production (AP) medium (10 g/L of glucose, 3 g/L of yeast extract, 3 g/L of malt extract, and 5 g/L of peptone, pH 5.5). Each flask was inoculated with a starter culture (5% v/v) and then incubated at 25 °C with 200 rpm shaking for 72 h. After incubation, the cells were harvested by centrifugation at 7830 rpm at 4 °C for 10 min, washed twice with deionized water, and centrifuged again. The cells were dried by lyophilization and weighed to obtain the DCW of the resultant cell biomass. The astaxanthin was extracted and quantified according to Li, Miao, Geng, Lu, Zhang, and Zeng [28].

Using the OFAAT method, astaxanthin production was optimized in *Rhodotorula* sp. CP72-2. The following parameters were varied: (1) type of carbon source (10 g/L of glucose, 10 g/L of sucrose, 10 g/L of fructose, or 10 g/L of maltose); (2) concentration of the selected carbon source (10, 20, 30, 40, or 50 g/L); (3) initial pH (4.5, 5.5, 6.5, 7.5, or 8.5) of the AP medium with an optimal carbon source and concentration; (4) incubation temperature at 15, 20, 25, 30, and 35 °C; and (5) incubation period at 1, 3, 5, and 7 days. The condition that resulted in the highest astaxanthin yield was selected for further experiments.

2.4. Statistical Analysis

All data were analyzed using One-way Analysis of Variance (ANOVA), and multiple comparison tests (Duncan's and Tukey's-tests) were performed using SPSS Statistic 22.0 software. Data were presented as mean ± standard deviation; $p < 0.05$ was considered statistically significant.

3. Results

3.1. Characteristics of Strain CP72-2

The study emphasizes the characterization, production, and optimization of astaxanthin and the genomic insights of a putatively new *Rhodotorula* sp. CP72-2 isolated from Thai *Calotropis gigantea*. The colony culture of strain CP72-2 on YM agar showed a distinct and characteristic appearance—pink-colored, butyrous, semi-shiny, globose-like morphology with an entire margin. The strain CP72-2′s carbon assimilation abilities were determined (Table S1). Characterizing its colony characteristics, individual morphology, and physiological and biochemical characteristics was consistent with the description of *Rhodotorula* species, as reported by Kurtzman and Robnett [29]. Based on the characteristics, it was suggested that CP72-2 belongs to the genus *Rhodotorula*. This information is relevant to identifying the strain and is consistent with the characteristics of *Rhodotorula* species.

Based on the 26S rRNA (LSU D1/D2 domain) gene sequencing, strain CP72-2 was found to be closely related to *Rhodotorula kratochvilovae*, with a 98% identity (595/604) (Table 1). According to the guideline of Kurtzman and Robnett [29], strains that differ by six or more nucleotide substitutions (>1%) should be considered different species. The term 'aff.' (species affinis) was used to indicate that the strain may be a potentially new species affiliated with, but not identical to, its closest known species [29].

Table 1. 26S rRNA gene sequence similarity (%) of the strain CP72-2 and nearest relatives.

Strain	Nearest Relatives	Similarity (%)	Length (bp)	Accession No.
CP72-2	*R. kratochvilovae* CBS 7436^T	98.35	604	NG_042345
	R. evergladensis CBS 10880^T	98.18	604	NG_057805
	R. araucariae CBS 6031^T	98.12	639	NG_058387
	R. glutinis CBS 20^T	97.57	1350	NG_055728
	R. babjevae CBS 7808^T	97.52	604	NG_042339

^{T}, indicated the type material strain.

Furthermore, the ANI value (Table S2) of the whole genomes between strain *Rhodotorula* sp. CP72-2 and *R. kratochvilovae* CBS 7436^T, *R. kratochvilovae* LS11, *R. kratochvilovae* YM25235, *R. babjevae* CBS 7808^T, *R. diobovata* UCD-FST 08-225, *R. glutinis* ZHK, *R. graminis* WP1, and *R. paludigena* CM33 were 83.1646%, 83.1079%, 83.0901%, 80.3203%, 80.2167%, 80.1658%, 80.0865%, and 79.3643%, respectively. The ANI value of the whole genomes between strain *Rhodotorula* sp. CP72-2 and closely related species were lower than the species boundary value (ANI < 95–96%) [30]. Based on these results and criteria, strain CP72-2 was considered a putatively new species.

3.2. Genomic Features of Strain CP72-2

This study proudly presents the results of the whole-genome analysis of *Rhodotorula* sp. CP72-2 to investigate the genomics features and gene annotation.

The assembled genome strain CP72-2 comprised 295 contigs, totaling 21,358,924 bp, and a high GC content of 64.90%. Furthermore, this assembly had an N50 value of 223,398 bp, an L50 value of 29 bp, and a maximum scaffold length of 748,751 bp. The program tRNAscan-SE identified 170 transfer RNAs (tRNAs) and 189 non-coding RNAs (ncRNAs) in the CP72-2 genome. The circular genomic map of *Rhodotorula* sp. CP72-2 is shown in Figure 1. Notably, the genome size of strain CP72-2 is consistent with other known red yeasts, including *R. graminis* WP1, *R. glutinis* ATCC 204091, *R. toruloides* NP11, and *Rhodotorula* sp. JG-1b has a genome size of approximatel 20–21 Mbp [31]. These results provide valuable insights into the genomic characteristics of red yeasts and contribute to our overall understanding of their biology.

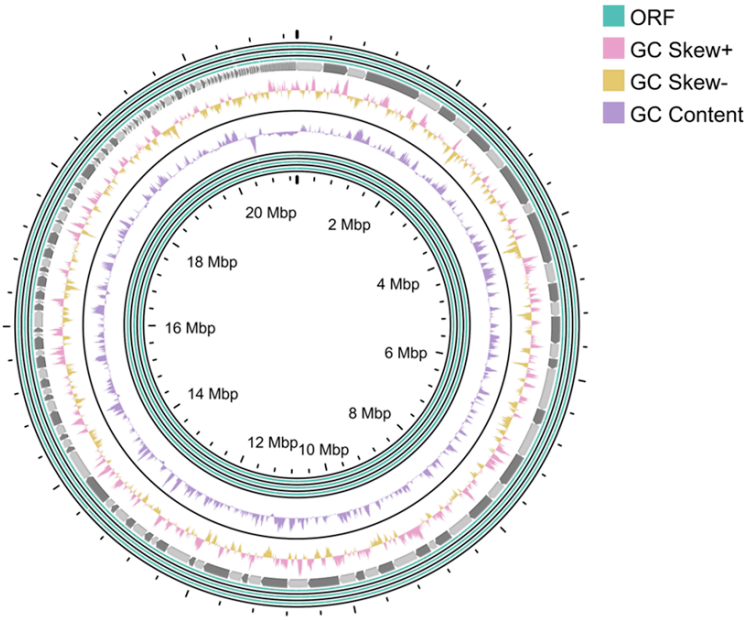

Figure 1. Circular genomic map of *Rhodotorula* sp. CP72-2. The information is indicated as follows: open reading frames (ORFs) (green), GC skew (+) (pink), GC skew (−) (yellow), and GC content (purple).

Furthermore, this study undertakes a comparative genomics investigation to unravel the genetic variations and peculiarities that distinguish *Rhodotorula* sp. CP72-2 from its four closely related species. The key objective of the study is to scrutinize the proteins that display similarities between protein sequences in the four yeast species (7670 proteins for *Rhodotorula* sp. CP72-2, 8257 proteins for *R. kratochvilovae* CBS 7436^T, 7509 proteins for *R. babjevae* CBS 7808^T, and 7518 proteins for *R. paludigena* CM33), as showcased in Figure 2. Notably, the investigation reveals that *Rhodotorula* sp. CP72-2, *R. kratochvilovae* CBS 7436^T, *R. babjevae* CBS 7808^T, and *R. paludigena* CM33 have 44, 89, 334, and 62 species/strains-specific proteins, respectively.

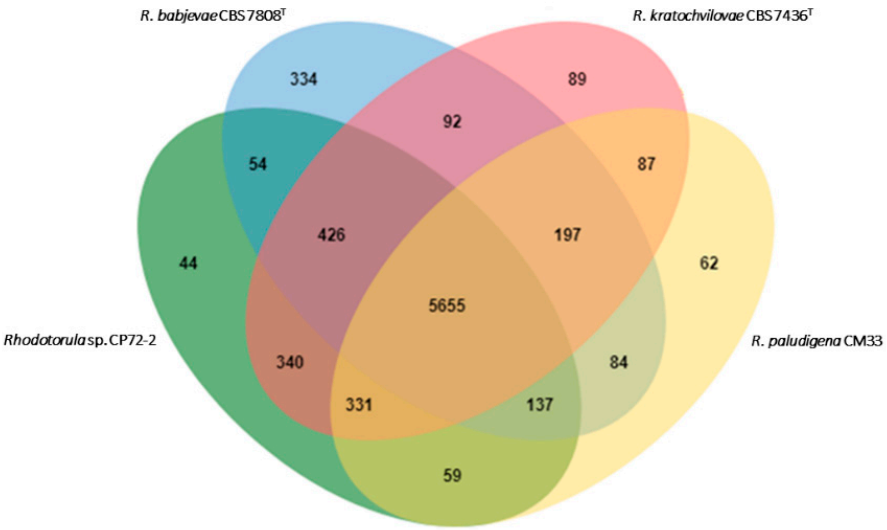

Figure 2. Venn diagram showing the shared/unique protein in *Rhodotorula* sp. CP72-2 and comparison with those in *R. kratochvilovae* CBS 7436^T, *R. babjevae* CBS 7808^T, and *R. paludigena* CM33.

Furthermore, the whole-genome sequence of strain CP72-2 annotated by the National Center for Biotechnology Information (NCBI) is estimated to have 6527 protein-coding genes and an average gene length of 1489.15 bp. In addition, 2291 genes involved in

KEGG metabolic pathway analysis were classified into five major categories: Metabolism Class (1043), followed by Genetic Information Processing (740), Environmental Information Processing (181), Organismal Systems (86), and Cellular Processes (241).

The genome of CP72-2 was analyzed using the dbCAN meta server, which identified 229 genes distributed among the five classes of the Carbohydrate-Active enZymes (CAZy) database, including 30 Auxiliary Activity (AA) genes, 18 Carbohydrate Esterase (CE) genes, two Carbohydrate-Binding Module (CBM) genes, 83 Glycoside Hydrolase (GH) genes, and 88 Glycosyltransferase (GT) genes. GH family enzymes in CP72-2 suggest its ability to break down cellulose and hemicellulose, major components of plant material, and use these complex carbohydrates for growth and survival [24]. The possession of GTs in CP72-2′s genome indicates its ability to synthesize the complex carbohydrates, such as glycoproteins and glycolipids, required for various biological functions [32]. The presence of CBMs in CP72-2′s genome suggests its ability to recognize and bind specific carbohydrates, such as plant cell walls and microbial surfaces [33]. AAs, crucial for breaking down plant biomass and recycling carbon and energy in the environment, were also identified in CP72-2′s genome, indicating its ability to degrade lignin in plant cell walls and use lignocellulose for growth [34]. All these impressive traits suggest that *Rhodotorula* sp. CP72-2 can potentially produce astaxanthin from lignocellulose and other waste resources from the agricultural industry.

3.3. Screening of Astaxanthin Production

Identifying and confirming astaxanthin production in strain CP72-2 is a significant finding. The accuracy and reliability of the results were ensured by using multiple techniques, including TLC, HPLC, and LC-MS.

TLC was initially used to confirm the presence of astaxanthin, with an R_f value of 0.28 (Figure 3A).

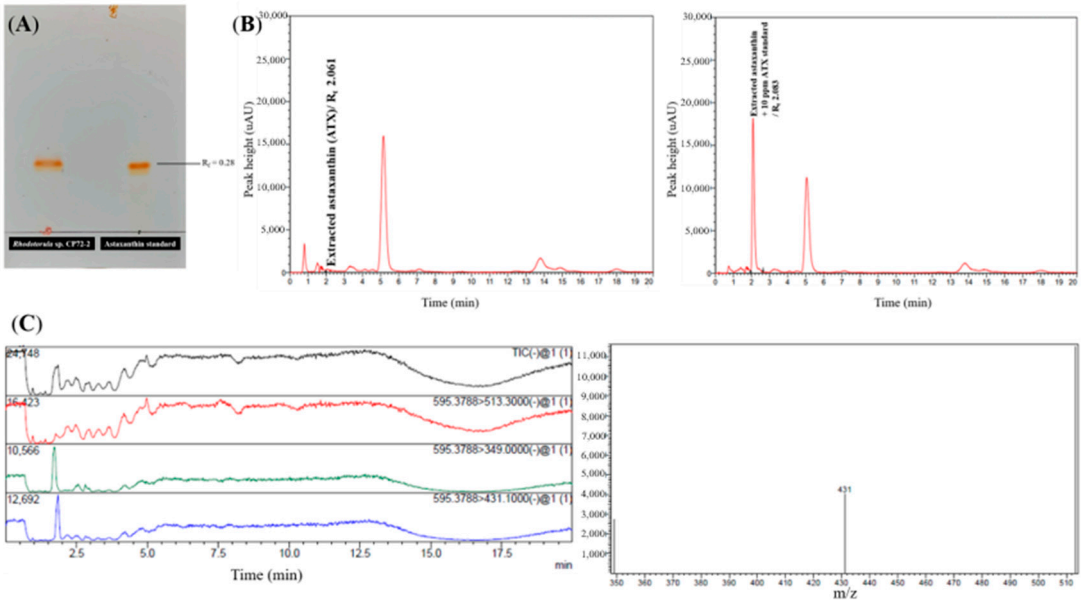

Figure 3. Thin Layer Chromatography (TLC) of an acetone extract of strain CP72-2 and astaxanthin standard (**A**); The determination HPLC chromatogram of extracted astaxanthin (non-spiked) and extracted astaxanthin + 10 ppm astaxanthin standard (spiked) of strain CP72-2 in DMSO (**B**); LC-MS chromatograms (MRM, negative scan mode) of extracted astaxanthin of strain CP72-2 in DMSO (**C**).

The HPLC chromatogram further confirmed the presence of astaxanthin, with the extracted astaxanthin of strain CP72-2 and the extracted astaxanthin containing 10 ppm of astaxanthin standard peak appearing at retention times of 2.063 and 2.083 min, respectively (Figure 3B).

Furthermore, mass spectrometric analysis was performed using MS/MS detection in negative scan mode. The extracted astaxanthin of strain CP72-2 in DMSO showed product ions (513.20, 430.75, 348.90) similar to the astaxanthin standard, which contained precursor ion (595.3822) and product ions (513.20 (CE = 25.0), 430.75 (CE = 12.0), 348.90 (CE = 48.0)) (Figure 3C). The optimization of the MS/MS parameter for astaxanthin detection was performed in MRM mode (MS/MS) by selecting a precursor ion of 595.3822 [M-H]- and three product ions of 513.2000, 430.7500, and 348.9000 with collision energy (CE) at 25.0, 12.0, and 48.0, respectively.

3.4. Astaxanthin Biosynthesis-Associated Genes from Strain CP72-2 Genome

This study also annotated putatively key enzyme genes associated with astaxanthin production in the CP72-2 genome. In the genome of strain CP72-2, the putative genes associated with astaxanthin biosynthesis were annotated and are listed in Table 2. The biosynthesis of astaxanthin is a complex process that involves the activity of several genes, including geranylgeranyl pyrophosphate synthase (*CrtE*), phytoene synthase/lycopene beta-cyclase (*CrtYB*), phytoene desaturase (*CrtI*), beta-carotene 4-ketolase/3-hydroxylase or astaxanthin synthase (*CrtS*), cytochrome P450 reductase (*CrtR*), beta-carotene/zeaxanthin 4-ketolase (*CrtW*), beta-carotene ketolase (*CrtO*), and beta-carotene hydroxylase (*CrtZ*).

Table 2. The putative candidate astaxanthin synthesis-associated genes from strain CP72-2 genome.

Biosynthetic Pathways	Putative Genes	Gene Product	Scaffold ID
Mevalonate	*ACAT*	Acetyl-CoA acetyltransferase (EC:2.3.1.9)	scaffold3.g328
	HMGCS	Hydroxymethylglutaryl-CoA synthase (EC:2.3.3.10)	scaffold118.g7197
	HMGCR	Hydroxymethylglutaryl-CoA reductase (EC:1.1.1.34)	scaffold69.g5807
	PMVK	Phosphomevalonate kinase (EC:2.7.4.2)	scaffold3.g296
	MVD	Diphosphomevalonate decarboxylase (EC:4.1.1.33)	scaffold42.g4393
Isoprene biosynthesis	*IDI*	Isopentenyl-diphosphate delta-isomerase (EC:5.3.3.2)	scaffold3.g272
	GGPS	Geranylgeranyl diphosphate synthase (EC:2.5.1.1 2.5.1.10 2.5.1.29)	scaffold33.g3627
	FDPS	Farnesyl diphosphate synthase (EC:2.5.1.1 2.5.1.10)	scaffold10.g1242
	CrtE	Geranylgeranyl pyrophosphate synthase	
Astaxanthin biosynthesis	*CrtYB*	Phytoene synthase/Lycopene beta-cyclase (EC:2.5.1.32 5.5.1.19)	scaffold16.g1927
	CrtI	Phytoene desaturase (EC:1.3.99.30)	scaffold16.g1930
Astaxanthin biosynthesis	*CrtS*	Beta-carotene 4-ketolase/3-hydroxylase (also known as astaxanthin synthase) (EC:1.14.99.63 1.14.15.24 1.14.99.-)	scaffold40.g4227
	CrtR	Cytochrome P450 reductase (EC:1.14.14.1 1.6.2.4)	scaffold80.g6179
	CrtW	Beta-carotene/zeaxanthin 4-ketolase (EC: EC:1.14.99.63 1.14.99.64)	scaffold38.g4135
	CrtO	Beta-carotene ketolase (EC:1.14.99.63)	scaffold16.g1930
	CrtZ	Beta-carotene hydroxylase (EC:1.14.13.-)	scaffold69.g5865

The important enzymes in astaxanthin production have been previously documented [35,36]. The process starts with the combination of dimethylallyl pyrophosphate (DMAPP) and three molecules of isopentenyl pyrophosphate (IPP) using GGPP synthase, resulting in the production of geranylgeranyl pyrophosphate (GGPP). The enzyme phytoene synthase (*CrtYB* gene) couples two molecules of GGPP to form phytoene. The phytoene desaturase (*CrtI* gene) introduces four double bonds in phytoene to produce lycopene. Lycopene cyclase (*CrtYB* gene) converts one of the ψ acyclic ends of lycopene into the β-ring to form γ-carotene, which is then converted into β-carotene. The process starts with the combination of dimethylallyl pyrophosphate (DMAPP) and three molecules of isopentenyl pyrophosphate (IPP) using GGPP synthase, resulting in the production of geranylgeranyl pyrophosphate (GGPP). The enzyme phytoene synthase (*CrtYB* gene) couples two molecules of GGPP to form phytoene. The phytoene desaturase (*CrtI* gene) introduces four double bonds in phytoene to produce lycopene. Lycopene cyclase (*CrtYB* gene) converts one of the ψ acyclic ends of lycopene into the β-ring to form γ-carotene, which is then converted into β-carotene. The conversion of β-carotene and γ-carotene into xanthophylls involves adding two 4-keto groups to the β-carotene molecule by ketolase activity and two 3-hydroxy groups by hydroxylase activity. These ketolase and hydroxylase activities are present in a single enzyme called astaxanthin synthetase (*CrtS*). To aid in the process, the cytochrome P450 reductase encoded by the *CrtR* gene acts as a helper protein for *CrtS* by providing electrons for substrate oxygenation [36]. The identification and cataloging of putative genes associated with astaxanthin biosynthesis, the prediction of their functions, and this putatively predictable pathway serve as a significant basis for the astaxanthin production in *Rhodotorula* sp. CP72-2 provides insights into the production of this valuable compound and a foundation for further research endeavors to enhance our understanding of the biosynthetic pathway of astaxanthin and develop novel bioprocesses for its production.

Following the in vitro confirmation of astaxanthin production and a comprehensive in silico investigation, it is unequivocally established that the *Rhodotorula* sp. CP72-2 strain possesses the ability to produce astaxanthin.

3.5. Optimization of Astaxanthin Production

The strain *Rhodotorula* sp. CP72-2 displays promise as a source for astaxanthin production, with an initial astaxanthin content of 202 ± 0.15 μg/g DCW and astaxanthin yield of 1.49 ± 0.0012 mg/L in YM medium after 72 h of cultivation at 25 °C and 200 rpm. To optimize production, a study was undertaken to investigate the effects of key factors, such as carbon sources and concentrations, pH, temperature, and incubation periods, on the growth and astaxanthin production of *Rhodotorula* sp. CP72-2.

3.5.1. Effects of Different Carbon Sources on Astaxanthin Production

The study examined the astaxanthin production of *Rhodotorula* sp. CP72-2 using four different carbon sources (glucose, maltose, fructose, and sucrose) at 10 g/L in an AP medium. The fermentation process was carried out at 25 °C and 200 rpm for 72 h. Surprisingly, the highest astaxanthin content (281.60 ± 0.54 μg/g DCW) and yield (1.73 ± 0.08 mg/L) were detected in the AP medium containing glucose (Figure 4A). Although the highest biomass (6.75 ± 0.07 g/L) was obtained in the AP medium containing sucrose, the content and yield of astaxanthin produced in this condition were significantly lower compared to the AP medium with glucose. As a result, glucose was identified as the optimal carbon source for further optimization of astaxanthin production.

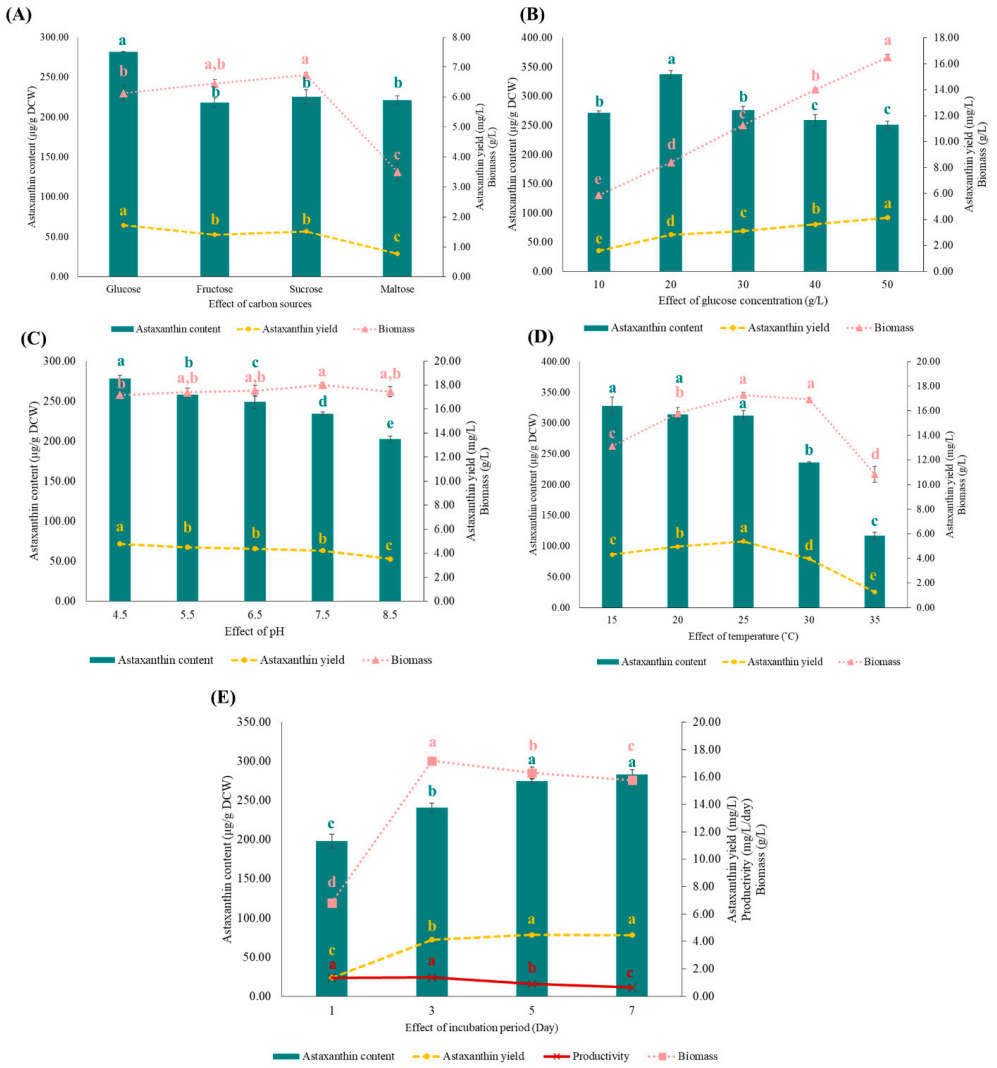

Figure 4. Effect of carbon sources (**A**), glucose concentration (**B**), pH (**C**), temperature (**D**), and incubation period (**E**) on the astaxanthin content (mg/g DCW), biomass (g/L), astaxanthin yield (mg/L), and productivity (mg/L/day) of strain CP72-2. All experiments were performed in triplicate, and the results were reported as the mean ± Standard Deviation (SD). Letters above the bars coded by different colors represent biomass, astaxanthin content, and astaxanthin concentration, respectively. According to Duncan's test ($p < 0.05$), the levels not connected by the same letter are significantly different. (For interpretation of the references to color in this figure legend, the reader is referred to the web version of this article).

Our research efforts revealed that *Rhodotorula* sp. CP72-2 exhibited an impressive ability to utilize diverse carbon sources and demonstrated vigorous growth. To achieve maximum astaxanthin production in strain CP72-2, this study meticulously optimized the medium composition and environmental factors. Our investigation into various carbon sources revealed that glucose medium was the most favorable for astaxanthin production, resulting in a maximum astaxanthin content of 281.60 ± 0.54 μg/g DCW and a maximum astaxanthin yield of 1.73 ± 0.08 mg/L. Conversely, the sucrose medium demonstrated the highest biomass production. The study of Wu and Yu [37] explained that glucose and sucrose are efficient carbon sources for promoting yeast growth and astaxanthin synthesis. Furthermore, the study observed that glucose and sucrose contributed to a moderate upregulation of carotenogenic genes such as *CrtI*, *CrtYB*, *CrtE*, and *CrtS* (or *ast*). This strongly supports the assertion that glucose is the preferred carbon source for astaxanthin synthesis.

3.5.2. Effect of Glucose Concentration on the Astaxanthin Production

The optimal glucose concentration for maximum astaxanthin content, yield, and biomass production of *Rhodotorula* sp. CP72-2 was investigated. To achieve this, various glucose concentrations (10, 20, 30, 40, and 50 g/L) were examined in an AP medium and incubated at 25 °C and 200 rpm for 72 h. The findings showed that an AP medium containing 20 g/L glucose was the best carbon source for maximum astaxanthin content (337.34 ± 6.97 μg/g DCW), as demonstrated in Figure 4B. However, the highest astaxanthin yield (4.14 ± 0.15 mg/L) and biomass (16.50 ± 0.229 g/L) were obtained when the medium contained 50 g/L glucose. Therefore, the AP medium containing 50 g/L glucose was used in further experiments.

Furthermore, *Rhodotorula* sp. CP72-2 was found to have the highest astaxanthin yield when cultured in an AP medium with an optimal glucose concentration of 50 g/L. Under 20 g/L glucose, astaxanthin content reached 337.34 ± 6.97 μg/g DCW. However, with 50 g/L glucose, the astaxanthin yield and biomass were significantly increased to 4.14 ± 0.15 mg/L and 16.50 ± 0.229 g/L, respectively. Miao et al. [38] conducted a study that supported the reduced astaxanthin content at 50 g/L glucose observed in our study. Their research explained that high glucose levels inhibited astaxanthin synthesis by repressing the lycopene-to-β-carotene and β-carotene-to-astaxanthin steps in the pathway. This inhibition was caused by the limited transfer of precursors (such as GGPP and phytoene) to carotenoids, which occurred at glucose concentrations exceeding 40 g/L. As a result, it appears that β-carotene synthesis is the limiting factor for astaxanthin synthesis at high glucose levels.

Additionally, high glucose may indicate a potential blockage of the astaxanthin synthesis pathway at the FPP-to-GGPP or GGPP-to-phytoene step. Moreover, as the glucose concentration rises beyond 40 g/L, there is a rapid decrease in *Crt*E expression, indicating that glucose primarily represses astaxanthin synthesis during the production of GGPP, phytoene, and lycopene. Moreover, it has been observed that the CP72-2 strain exhibits the crabtree effect, characterized by the overproduction of fermentation byproducts. This phenomenon significantly impedes astaxanthin synthesis when glucose concentrations exceed 40 g/L, consistent with previous findings [39,40]. These results suggest that optimizing the glucose concentration is crucial to achieving maximum astaxanthin yield, as a balance must be struck between astaxanthin synthesis and precursor transfer.

3.5.3. Effect of Initial pH of the AP Medium on the Astaxanthin Production

The impact of initial pH on astaxanthin production was investigated in an optimum AP medium supplemented with 50 g/L glucose. The fermentation was carried out at 25 °C and 200 rpm for three days, with pH levels ranging from 4.5 to 8.5. The results revealed that the highest astaxanthin content and yield were achieved at pH 4.5, with values of 277.94 ± 4.29 μg/g DCW and 4.78 ± 0.14 mg/L, respectively (Figure 4C). The highest biomass of 18.02 ± 0.15 g/L was observed at pH 7.5, while acidic and alkaline pH levels resulted in decreased biomass. Therefore, a pH of 4.5 was selected as the optimal initial pH of the AP medium for maximum astaxanthin production by *Rhodotorula* sp. CP72-2 in the AP medium supplemented with 50 g/L glucose.

The production of astaxanthin by *Rhodotorula* sp. CP72-2 was found to be affected by the pH of the fermentation medium. Reducing the initial pH value from 8.5 to 4.5 led to a rise in astaxanthin yield from 3.53 ± 0.07 to 4.78 ± 0.14 mg/L. These findings suggest that an acidic environment pH of 4.5 promotes astaxanthin synthesis in strain CP72-2. Hence, pH stress has emerged as a promising approach to stimulate astaxanthin production in cellular environments. The maximum astaxanthin content and yield were obtained at pH 4.5. Therefore, the optimal pH for the astaxanthin content and yield of *Rhodotorula* sp. CP72-2 was found to be 4.5. The results of this research align with earlier studies that indicated an acidic pH as the optimum condition for astaxanthin production [41–43]. These results underscore the importance of pH control as a critical factor in optimizing astaxanthin production by strain CP72-2.

3.5.4. Effect of Temperature on the Astaxanthin Production

The production of astaxanthin by *Rhodotorula* sp. CP72-2 was investigated at various incubation temperatures (15, 20, 25, 30, and 35 °C). To determine the optimal temperature, the astaxanthin yield of strain CP72-2 was compared when grown in an AP medium supplemented with 50 g/L of glucose and at pH 4.5. The results revealed that the greatest astaxanthin yield (5.39 ± 0.21 mg/L), biomass (17.28 ± 0.21 g/L), and astaxanthin content (311.99 ± 8.69 µg/gDCW) were obtained at an incubation temperature of 25 °C (Figure 4D). Thus, this temperature was considered the optimal temperature for astaxanthin production by *Rhodotorula* sp. CP72-2.

Alterations in various biosynthetic pathways, including those involved in carotenoid biosynthesis, can be attributed to temperature changes. The impact of temperature on carotenoid synthesis is contingent on the species- and/or strain-specific characteristics and can result in fluctuations in the yield of produced carotenoids [44]. However, the effect of temperature on carotenoid production can indeed vary among different strains [41,45–47]. In our study, we discovered a unique optimal temperature for the growth and astaxanthin production of strain CP72-2, which was determined to be 25 °C. It is worth noting that our findings contrast with the investigation conducted by Polulyakh et al. [48], in which they observed high astaxanthin content (85%) in *Phaffia rhodozyma* when cultivated at 20 °C. Hence, maintaining optimal temperature is crucial for cell metabolism. It regulates the catabolic rate of enzymes and the half-life of proteins, which can directly impact the cell's metabolic processes [49]. In addition, the impact of temperature on astaxanthin production may be attributed to the temperature-dependent nature of the enzymatic activities involved in its biosynthesis [50]. Moreover, environmental changes influence various essential genes linked to astaxanthin synthesis [49]. Hayman et al. [51] reported that temperature influences the regulation of two crucial enzymes involved in carotenoid biosynthesis: beta-carotene synthetase and torulene synthetase. These results highlight the critical role of incubation temperature as a key determinant of optimal astaxanthin production in this strain and underscore the importance of temperature control during cultivation.

3.5.5. Effect of Incubation Period on the Astaxanthin Production

The aim of this study was to investigate the impact of the incubation period on astaxanthin production in *Rhodotorula* sp. CP72-2. The strain was grown in AP medium, supplemented with 50 g/L of glucose, and incubated at 25 °C and 200 rpm, with the incubation period varied from 1 to 7 days. The results demonstrated that the highest astaxanthin content (283.34 ± 6.26 µg/g DCW) and astaxanthin yield (4.48 ± 0.15 mg/L) were obtained at 7 and 5 days of the incubation period, respectively (Figure 4E). However, the greatest astaxanthin productivity (1.38 ± 0.04 mg/L/day) and biomass (17.17 ± 0.19 g/L) were observed on day 3, and it was significantly different from the productivity on day 5 (0.90 ± 0.03 mg/L/day) and day 7 (0.64 ± 0.01 mg/L/day). Therefore, the optimal incubation period for astaxanthin production in *Rhodotorula* sp. CP72-2 was determined to be three days. Another factor influencing astaxanthin production was the incubation period. Carotenoid biosynthesis in yeasts begins in the late logarithmic phase and progresses to the stationary phase. The maximum astaxanthin yield was obtained at five days of the incubation (4.48 ± 0.15 mg/L); however, the maximum astaxanthin productivity (mg/L/day) of *Rhodotorula* sp. CP72-2 was accessed at an incubation period of three days. According to Naghavi et al. [52], the optimal incubation period for maximum carotenoid biosynthesis of *R. slooffiae* was 72 h. Based on the result of astaxanthin productivity, it could be summarized that the optimal incubation period for astaxanthin production in *Rhodotorula* sp. CP72-2 was three days. Therefore, careful monitoring and control of the incubation period are crucial in optimizing the astaxanthin production process.

In this work, the maximum astaxanthin productivity produced by *Rhodotorula* sp. CP72-2 in the optimized AP medium at optimal condition was 1.38 ± 0.04 mg/L/day

(astaxanthin content of 240.64 ± 5.82 μg/g DCW). It is noteworthy that further extension of the incubation time beyond three days reduced the biomass of strain CP72-2.

4. Conclusions

After considering the previous discussion, it is clear that *Rhodotorula* sp. CP72-2 holds immense potential for producing valuable carotenoids with countless applications. The recently discovered strain CP72-2 (accession number: 26S rRNA: OP547513; WGS project accession: PRJNA938253) is a putatively new addition to the yeast species found in Thailand's Prachinburi province and one of the few species reported from other parts of the world. Notably, strain CP72-2 has shown the ability to synthesize astaxanthin, a highly sought-after compound across various industries worldwide. Optimization experiments have determined that the best conditions for producing astaxanthin from strain CP72-2 involve using 50 g/L glucose, initially setting the pH to 4.5, incubating at 25 °C, and agitating at 200 rpm for three days. These conditions resulted in an impressive astaxanthin content of 240.64 ± 5.82 μg/g DCW, 17.17 g/L biomass, 4.13 ± 0.133 mg/L astaxanthin yield, and a productivity rate of 1.38 ± 0.04 mg/L/day astaxanthin. Furthermore, the whole-genome sequencing analysis of strain CP72-2 was annotated. Several putative candidate genes were explored, including *CrtE*, *CrtYB*, *CrtI*, *CrtS*, *CrtR*, *CrtW*, *CrtO*, and *CrtZ*, associated with astaxanthin biosynthesis. These findings provide a solid foundation for future research on characterizing, optimizing, and understanding the genomic insights of astaxanthin production from strain CP72-2.

Supplementary Materials: The following supporting information can be downloaded at: https://www.mdpi.com/article/10.3390/fermentation9060501/s1, Table S1: Carbon assimilation of strain CP72-2; Table S2: ANI (%) values between the draft genomes of the *Rhodotorula* sp. CP72-2; *R. kratochvilovae* CBS 7436^T; *R. kratochvilovae* LS11; *R. kratochvilovae* YM25235; *R. babjevae* CBS 7808^T; *R. diobovata* UCD-FST 08-225; *R. glutinis* ZHK; *R. graminis* WP1; and *R. paludigena* CM33. Table S3: The effect of different carbon sources on astaxanthin production and growth of *Rhodotorula* sp. CP72-2. Table S4: The effect of glucose concentration on astaxanthin production and growth of *Rhodotorula* sp. CP72-2. Table S5: The effect of pH on astaxanthin production and growth of *Rhodotorula* sp. CP72-2. Table S6: The effect of temperature on astaxanthin production and growth of *Rhodotorula* sp. CP72-2. Table S7: The effect of incubation period on astaxanthin production and growth of *Rhodotorula* sp. CP72-2.

Author Contributions: E.K., conceptualization, data curation, formal analysis, methodology, writing—original draft, writing—review and editing; N.T., conceptualization, methodology, writing—review and editing; S.P., conceptualization, data curation, formal analysis, methodology; P.R., conceptualization, data curation, formal analysis, writing—review and editing; B.S., conceptualization, methodology, writing—review and editing; W.T., data curation, formal analysis; S.T. (Somphob Thompho), data curation, formal analysis; W.M., conceptualization, methodology, writing—review and editing; S.T. (Somboon Tanasupawat), conceptualization, funding acquisition, project administration, resources, supervision, writing—review and editing. All authors have read and agreed to the published version of the manuscript.

Funding: This research was funded by Thailand Science Research and Innovation Fund Chulalongkorn University (CU_FRB65_hea (51)_060_33_04). Furthermore, this study thanks the Pharmaceutical Research Instrument Center, Faculty of Pharmaceutical Sciences, Chulalongkorn University, for providing research facilities.

Institutional Review Board Statement: Not applicable.

Informed Consent Statement: Not applicable.

Data Availability Statement: The 26S rRNA gene sequence and the draft genome of *Rhodotorula* sp. CP72-2 were deposited in NCBI (accession no.: OP547513 and PRJNA938253, respectively).

Conflicts of Interest: The authors declare no conflict of interest.

References

1. Allahkarami, S.; Sepahi, A.A.; Hosseini, H.; Razavi, M.R. Isolation and identification of carotenoid-producing *Rhodotorula* sp. from Pinaceae forest ecosystems and optimization of in vitro carotenoid production. *Biotechnol. Rep.* **2021**, *32*, e00687. [CrossRef] [PubMed]
2. Dursun, D.; Dalgıç, A.C. Optimization of astaxanthin pigment bioprocessing by four different yeast species using wheat wastes. *Biocatal. Agric. Biotechnol.* **2016**, *7*, 1–6. [CrossRef]
3. Visser, H.; van Ooyen, A.J.J.; Verdoes, J.C. Metabolic engineering of the astaxanthin-biosynthetic pathway of *Xanthophyllomyces dendrorhous*. *FEMS Yeast Res.* **2003**, *4*, 221–231. [CrossRef] [PubMed]
4. Guerin, M.; Huntley, M.E.; Olaizola, M. *Haematococcus* astaxanthin: Applications for human health and nutrition. *Trends Biotechnol.* **2003**, *21*, 210–216. [CrossRef]
5. Rodríguez-Sáiz, M.; de la Fuente, J.L.; Barredo, J.L. *Xanthophyllomyces dendrorhous* for the industrial production of astaxanthin. *Appl. Microbiol. Biotechnol.* **2010**, *88*, 645–658. [CrossRef]
6. Ambati, R.R.; Moi, P.S.; Ravi, S.; Aswathanarayana, R.G. Astaxanthin: Sources, extraction, stability, biological activities and its commercial applications—A review. *Mar. Drugs* **2014**, *12*, 128–152. [CrossRef]
7. Casella, P.; Iovine, A.; Mehariya, S.; Marino, T.; Musmarra, D.; Molino, A. Smart method for carotenoids characterization in *Haematococcus pluvialis* red phase and evaluation of astaxanthin thermal stability. *Antioxidants* **2020**, *9*, 422. [CrossRef]
8. Kikukawa, H.; Shimizu, C.; Hirono-Hara, Y.; Hara, K.Y. Screening of plant oils promoting growth of the red yeast *Xanthophyllomyces dendrorhous* with astaxanthin and fatty acid production. *Biocatal. Agric. Biotechnol.* **2021**, *35*, 102101. [CrossRef]
9. Kim, J.-H.; Kang, S.-W.; Kim, S.-W.; Chang, H.-I. High-level production of astaxanthin by *Xanthophyllomyces dendrorhous* mutant JH1 using statistical experimental designs. *Biosci. Biotechnol. Biochem.* **2005**, *69*, 1743–1748. [CrossRef]
10. Kurtzman, C.P.; Fell, J.W.; Boekhout, T. *The Yeasts: A Taxonomic Study*; Elsevier: Amsterdam, The Netherlands, 2011.
11. O'Donnell, K.; Gray, L.E. Phylogenetic relationships of the soybean sudden death syndrome pathogen *Fusarium solani* f. sp. *phaseoli* inferred from rDNA sequence data and PCR primers for its identification. *Mol. Plant-Microbe Interact. MPMI* **1995**, *8*, 709–716. [CrossRef]
12. Zerbino, D.R.; McEwen, G.K.; Margulies, E.H.; Birney, E. Pebble and rock band: Heuristic resolution of repeats and scaffolding in the velvet short-read de novo assembler. *PLoS ONE* **2009**, *4*, e8407. [CrossRef]
13. Zerbino, D.R.; Birney, E. Velvet: Algorithms for de novo short read assembly using de Bruijn graphs. *Genome Res.* **2008**, *18*, 821–829. [CrossRef]
14. Boetzer, M.; Henkel, C.V.; Jansen, H.J.; Butler, D.; Pirovano, W. Scaffolding pre-assembled contigs using SSPACE. *Bioinformatics* **2011**, *27*, 578–579. [CrossRef] [PubMed]
15. Hunt, M.; Newbold, C.; Berriman, M.; Otto, T.D. A comprehensive evaluation of assembly scaffolding tools. *Genome Biol.* **2014**, *15*, R42. [CrossRef] [PubMed]
16. Boetzer, M.; Pirovano, W. Toward almost closed genomes with GapFiller. *Genome Biol.* **2012**, *13*, R56. [CrossRef]
17. Stanke, M.; Schöffmann, O.; Morgenstern, B.; Waack, S. Gene prediction in eukaryotes with a generalized hidden Markov model that uses hints from external sources. *BMC Bioinform.* **2006**, *7*, 62. [CrossRef] [PubMed]
18. Lowe, T.M.; Eddy, S.R. tRNAscan-SE: A program for improved detection of transfer RNA genes in genomic sequence. *Nucleic Acids Res.* **1997**, *25*, 955–964. [CrossRef]
19. Jain, C.; Rodriguez-R, L.M.; Phillippy, A.M.; Konstantinidis, K.T.; Aluru, S. High throughput ANI analysis of 90K prokaryotic genomes reveals clear species boundaries. *Nat. Commun.* **2018**, *9*, 5114. [CrossRef]
20. Grant, J.R.; Stothard, P. The CGView Server: A comparative genomics tool for circular genomes. *Nucleic Acids Res.* **2008**, *36*, W181–W184. [CrossRef]
21. Xu, L.; Dong, Z.; Fang, L.; Luo, Y.; Wei, Z.; Guo, H.; Zhang, G.; Gu, Y.Q.; Coleman-Derr, D.; Xia, Q. OrthoVenn2: A web server for whole-genome comparison and annotation of orthologous clusters across multiple species. *Nucleic Acids Res.* **2019**, *47*, W52–W58. [CrossRef]
22. Kanehisa, M.; Sato, Y.; Morishima, K. BlastKOALA and GhostKOALA: KEGG tools for functional characterization of genome and metagenome sequences. *J. Mol. Biol.* **2016**, *428*, 726–731. [CrossRef]
23. Aramaki, T.; Blanc-Mathieu, R.; Endo, H.; Ohkubo, K.; Kanehisa, M.; Goto, S.; Ogata, H. KofamKOALA: KEGG Ortholog assignment based on profile HMM and adaptive score threshold. *Bioinformatics* **2020**, *36*, 2251–2252. [CrossRef]
24. Cantarel, B.L.; Coutinho, P.M.; Rancurel, C.; Bernard, T.; Lombard, V.; Henrissat, B. The Carbohydrate-Active EnZymes database (CAZy): An expert resource for glycogenomics. *Nucleic Acids Res.* **2009**, *37*, D233–D238. [CrossRef]
25. Zhang, H.; Yohe, T.; Huang, L.; Entwistle, S.; Wu, P.; Yang, Z.; Busk, P.K.; Xu, Y.; Yin, Y. dbCAN2: A meta server for automated carbohydrate-active enzyme annotation. *Nucleic Acids Res.* **2018**, *46*, W95–W101. [CrossRef]
26. Ushakumari, U.N.; Ramanujan, R. Isolation of astaxanthin from marine yeast and study of its pharmacological activity. *Int. Curr. Pharm. J.* **2013**, *2*, 67–69. [CrossRef]
27. Sharma, R.; Ghoshal, G. Optimization of carotenoids production by *Rhodotorula mucilaginosa* (MTCC-1403) using agro-industrial waste in bioreactor: A statistical approach. *Biotechnol. Rep.* **2020**, *25*, e00407. [CrossRef] [PubMed]
28. Li, Y.; Miao, F.; Geng, Y.; Lu, D.; Zhang, C.; Zeng, M. Accurate quantification of astaxanthin from *Haematococcus* crude extract spectrophotometrically. *Chin. J. Oceanol. Limnol.* **2012**, *30*, 627–637. [CrossRef]

29. Kurtzman, C.P.; Robnett, C.J. Identification and phylogeny of ascomycetous yeasts from analysis of nuclear large subunit (26S) ribosomal DNA partial sequences. *Antonie Leeuwenhoek* **1998**, *73*, 331–371. [CrossRef] [PubMed]
30. Libkind, D.; Čadež, N.; Opulente, D.A.; Langdon, Q.K.; Rosa, C.A.; Sampaio, J.P.; Gonçalves, P.; Hittinger, C.T.; Lachance, M.A. Towards yeast taxogenomics: Lessons from novel species descriptions based on complete genome sequences. *FEMS Yeast Res.* **2020**, *20*, foaa042. [CrossRef]
31. Fakankun, I.; Fristensky, B.; Levin, D.B. Genome sequence analysis of the oleaginous yeast, *Rhodotorula diobovata*, and comparison of the carotenogenic and oleaginous pathway genes and gene products with other oleaginous yeasts. *J. Fungi* **2021**, *7*, 320. [CrossRef]
32. Lombard, V.; Ramulu, H.G.; Drula, E.; Coutinho, P.M.; Henrissat, B. The carbohydrate-active enzymes database (CAZy) in 2013. *Nucleic Acids Res.* **2014**, *42*, D490–D495. [CrossRef] [PubMed]
33. Boraston, A.B.; Bolam, D.N.; Gilbert, H.J.; Davies, G.J. Carbohydrate-binding modules: Fine-tuning polysaccharide recognition. *Biochem. J.* **2004**, *382*, 769–781. [CrossRef]
34. Levasseur, A.; Drula, E.; Lombard, V.; Coutinho, P.M.; Henrissat, B. Expansion of the enzymatic repertoire of the CAZy database to integrate auxiliary redox enzymes. *Biotechnol. Biofuels* **2013**, *6*, 1–14. [CrossRef]
35. Li, C.-J.; Zhao, D.; Cheng, P.; Zheng, L.; Yu, G.-H. Genomics and lipidomics analysis of the biotechnologically important oleaginous red yeast *Rhodotorula glutinis* ZHK provides new insights into its lipid and carotenoid metabolism. *BMC Genom* **2020**, *21*, 1–16. [CrossRef] [PubMed]
36. Barredo, J.L.; García-Estrada, C.; Kosalkova, K.; Barreiro, C. Biosynthesis of astaxanthin as a main carotenoid in the heterobasidiomycetous yeast *Xanthophyllomyces dendrorhous*. *J. Fungi* **2017**, *3*, 44. [CrossRef] [PubMed]
37. Wu, W.; Yu, X. Effect of different carbon source on expression of carotenogenic genes and astaxanthin production in *Xanthophyllomyces dendrorhous*. *Adv. J. Food Sci. Technol.* **2013**, *5*, 1375–1379. [CrossRef]
38. Miao, L.; Chi, S.; Wu, M.; Liu, Z.; Li, Y. Deregulation of phytoene-β-carotene synthase results in derepression of astaxanthin synthesis at high glucose concentration in *Phaffia rhodozyma* astaxanthin-overproducing strain MK19. *BMC Microbiol.* **2019**, *19*, 133. [CrossRef]
39. Reynders, M.B.; Rawlings, D.E.; Harrison, S.T.L. Demonstration of the Crabtree effect in *Phaffia rhodozyma* during continuous and fed-batch cultivation. *Biotechnol. Lett.* **1997**, *19*, 549–552. [CrossRef]
40. Sandmann, G. Carotenoid biosynthesis in microorganisms and plants. *Eur. J. Biochem.* **1994**, *223*, 7–24. [CrossRef]
41. Johnson, E.A.; Lewis, M.J. Astaxanthin formation by the yeast *Phaffia rhodozyma*. *J. Gen. Microbiol.* **1979**, *115*, 173–183. [CrossRef]
42. Meyer, P.S.; Du Preez, J.C. Effect of culture conditions on astaxanthin production by a mutant of *Phaffia rhodozyma* in batch and chemostat culture. *Appl. Microbiol. Biotechnol.* **1994**, *40*, 780–785. [CrossRef]
43. Fang, T.J.; Cheng, Y.-S. Improvement of astaxanthin production by *Phaffia rhodozyma* through mutation and optimization of culture conditions. *J. Ferment Bioeng.* **1993**, *75*, 466–469. [CrossRef]
44. Frengova, G.I.; Beshkova, D.M. Carotenoids from *Rhodotorula* and *Phaffia*: Yeasts of biotechnological importance. *J. Ind. Microbiol. Biotechnol.* **2009**, *36*, 163. [CrossRef] [PubMed]
45. Martin, A.M.; Acheampong, E.; Patel, T.R.; Chornet, E. Study of growth parameters for *Phaffia rhodozyma* cultivated in peat hydrolysates. *Appl. Biochem. Biotechnol.* **1992**, *37*, 235–241. [CrossRef]
46. Martin, A.M.; Lu, C.; Patel, T.R. Growth parameters for the yeast *Rhodotorula rubra* grown in peat extracts. *J. Ferment. Bioeng.* **1993**, *76*, 321–325. [CrossRef]
47. Kusdiyantini, E.; Gaudin, P.; Goma, G.; Blanc, P.J. Growth kinetics and astaxanthin production of *Phaffia rhodozyma* on glycerol as a carbon source during batch fermentation. *Biotechnol. Lett.* **1998**, *20*, 929–934. [CrossRef]
48. Polulyakh, O.V.; Podoprigora, O.I.; Eliseev, S.A.; Ershov, Y.U.V.; Bykhovskii, V.Y.; Dmitrovskii, A.A. Biosynthesis of torulene and torularhodin by the yeast *Phaffia rhodozyma*. *Appl. Biochem. Microbiol. USA* **1992**, *27*, 411–414.
49. Ren, Y.; Deng, J.; Huang, J.; Wu, Z.; Yi, L.; Bi, Y.; Chen, F. Using green alga *Haematococcus pluvialis* for astaxanthin and lipid co-production: Advances and outlook. *Bioresour. Technol.* **2021**, *340*, 125736. [CrossRef]
50. Xiao, R.; Li, X.; Leonard, E.; Tharayil, N.; Zheng, Y. Investigation on the effects of cultivation conditions, fed-batch operation, and enzymatic hydrolysate of corn stover on the astaxanthin production by *Thraustochytrium striatum*. *Algal Res.* **2019**, *39*, 101475. [CrossRef]
51. Hayman, E.P.; Yokoyama, H.; Chichester, C.O.; Simpson, K.L. Carotenoid biosynthesis in *Rhodotorula glutinis*. *J. Bacteriol.* **1974**, *120*, 1339–1343. [CrossRef]
52. Naghavi, F.S.; Hanachi, P.; Soudi, M.R.; Saboora, A.; Ghorbani, A. Evaluation of the relationship between the incubation time and carotenoid production in *Rhodotorula slooffiae* and *R. mucilaginosa* isolated from leather tanning wastewater. *Iran J. Basic Med. Sci.* **2013**, *16*, 1114. [CrossRef]